

College of Arts and Sciences



Drexel E-Repository and Archive (iDEA)
<http://idea.library.drexel.edu/>

Drexel University Libraries
www.library.drexel.edu

The following item is made available as a courtesy to scholars by the author(s) and Drexel University Library and may contain materials and content, including computer code and tags, artwork, text, graphics, images, and illustrations (Material) which may be protected by copyright law. Unless otherwise noted, the Material is made available for non profit and educational purposes, such as research, teaching and private study. For these limited purposes, you may reproduce (print, download or make copies) the Material without prior permission. All copies must include any copyright notice originally included with the Material. **You must seek permission from the authors or copyright owners for all uses that are not allowed by fair use and other provisions of the U.S. Copyright Law.** The responsibility for making an independent legal assessment and securing any necessary permission rests with persons desiring to reproduce or use the Material.

Please direct questions to archives@drexel.edu

Asymmetric band profile of the Soret band of deoxymyoglobin is caused by electronic and vibronic perturbations of the heme group rather than by a doming deformation

Reinhard Schweitzer-Stenner,^{a)} John Paul Gorden, and Andrew Hagarman
Department of Chemistry, Drexel University, Philadelphia, PA 19104, USA

(Received 5 June 2007; accepted 1 August 2007; published online 4 October 2007)

We measured the Soret band of deoxymyoglobin (deoxyMb), myoglobin cyanide (MbCN), and aquo-metmyoglobin (all from horse heart) with absorption and circular dichroism (CD) spectroscopies. A clear non-coincidence was observed between the absorption and CD profiles of deoxyMb and MbCN, with the CD profiles red- and blueshifted with respect to the absorption band position, respectively. On the contrary, the CD and absorption profiles of aquametMb were nearly identical. The observed noncoincidence indicates a splitting of the excited B state due to heme-protein interactions. CD and absorption profiles of deoxyMb and MbCN were self-consistently analyzed by employing a perturbation approach for weak vibronic coupling as well as the relative intensities and depolarization ratios of seven bands in the respective resonance Raman spectra measured with B -band excitation. The respective B_y component was found to dominate the observed Cotton effect of both myoglobin derivatives. The different signs of the noncoincidences between CD and absorption bands observed for deoxyMb and MbCN are due to different signs of the respective matrix elements of A_{1g} electronic interstate coupling, which reflects an imbalance of Gouterman's 50:50 states. The splitting of the B band reflects contributions from electronic and vibronic perturbations of B_{1g} symmetry. The results of our analysis suggest that the broad and asymmetric absorption band of deoxyMb results from this band splitting rather than from its dependence on heme doming. Thus, we are able to explain recent findings that the temperature dependences of CO rebinding to myoglobin and the Soret band profile are uncorrelated [Ormos *et al.*, Proc. Natl. Acad. Sci U.S.A. **95**, 6762 (1998)]. © 2007 American Institute of Physics. [DOI: 10.1063/1.2775931]

INTRODUCTION

Over the past 30 years, myoglobin has been utilized frequently as a laboratory to study the underlying physics of protein structure and function.¹⁻⁷ Myoglobin is a monomeric protein with a molecular weight of 16.7 kDa that contains a Fe-protoporphyrin molecule as its prosthetic group. It binds oxygen and other small ligands such as carbon monoxide reversibly. Numerous studies have shown that ligand binding dynamics are more complex than initially expected in that the binding ligand probes a large number of different conformational substates with slightly different activation enthalpies.^{2,8-11} While fluctuation between substates is fast at room temperature, it slows down at temperatures below the glass transition of the solvent (water/glycerol), so that the sample becomes inhomogeneous.¹¹

The doming of the heme group, which involves an out-of-plane displacement of the central iron atom, has been considered as the decisive kinetic coordinate, the distribution of which determines the enthalpy distribution encountered by the binding ligand.¹⁰⁻¹² However, this notion was recently challenged by Ormos *et al.* based on a very detailed kinetic study on CO rebinding to myoglobin.¹³ They found that the

kinetics of oxygen rebinding at cryogenic temperatures does not depend on the coordinates that affect the respective band profile of the Soret band of the deoxystate. Since theoretical modeling by Šrajcar *et al.* suggested that the broad and asymmetric band profile of this band reflects a Gaussian distribution of substates along the doming coordinate,¹⁴ Ormos *et al.* concluded that the doming coordinate is not significantly influencing the activation enthalpy of ligand rebinding. This result was surprising in view of the compelling evidence to the contrary.^{10,11,14} However, the conclusion of Ormos *et al.*¹³ depends on the validity of the band modeling of Šrajcar *et al.*,¹⁴ which has been more recently questioned by Franzen,¹⁵ who invoked vibronic coupling between the B state and an excited charge transfer state associated with band III in the near-infrared region of the heme absorption spectrum to explain the magnetic circular dichroism (MCD) spectrum of deoxyMb in the Soret band region. Franzen argues that this coupling lifts the degeneracy of the excited B state, and that it is this splitting rather than heme doming which is mainly responsible for the asymmetric and broad profile of the Soret band. If this is true, the results of Ormos *et al.*¹³ would not argue against an influence of heme doming on the kinetics of ligand rebinding. Since finding a physically correct model for the profile of the Soret band is apparently important for the understanding of the ligand binding process, we decided to investigate the composition of the

^{a)} Author to whom correspondence should be addressed.
 Tel.: (215) 895-2268; Fax: (215) 895-1265.
 Electronic mail: rschweitzer-stenner@drexel.edu

Soret band by subjecting its absorption and CD profiles to a self-consistent vibronic analysis based on the relative intensities and depolarization ratios of prominent resonance Raman bands recorded with Soret excitation. As recently shown by Dragomir *et al.*,¹⁶ CD spectra, in some circumstances, can be utilized to probe and quantify the splitting of Q and B bands of heme proteins, which do not appear in the absorption spectrum even at cryogenic temperatures. For the sake of comparison, we also use the above spectroscopies to investigate the Soret bands of myoglobin cyanide (MbCN) and high spin ferric aqua-metmyoglobin (aquametMb). Our results identify electronic and vibronic perturbations as the decisive determinants of the Soret band profile of heme proteins with a pentacoordinated ferrous heme.

MATERIALS AND METHODS

Materials

Horse heart metMb was purchased from Sigma-Aldrich Co. (St. Louis, MO) with no further purification and dissolved in 1 mM phosphate buffer solution. To obtain the MbCN, KCN, obtained from Fisher Scientific (Pittsburg, PA), was added to a stock solution of metMb at a ratio of 1.5:1. Metmyoglobin was reduced with sodium dithionite, obtained from Fluka (Sigma-Aldrich Co.), in stoichiometric excess before acquisition to obtain the deoxystate. 50 μ M solutions of myoglobin were prepared for CD and absorption measurements.

Methods

Spectra in the range of the Soret band were measured from 350 to 550 nm in digital form with a JASCO J-810 spectropolarimeter (Jasco, Inc.) purged with N_2 . Twenty accumulations were taken using a 5 nm bandwidth, a 50 nm/min scanning speed, and a 0.2 nm data pitch. Additionally, a background subtraction was carried out for all spectra using similar parameters. A constant temperature of 20 °C was controlled by a Peltier cooling system (± 1 °C). All spectra were measured in a 1.0 cm quartz cell. The pH was measured before and after measurement to ensure that no change in pH occurred during the measurement. Nonlinear base lines were subtracted from the spectra with MULTIFIT.¹⁷ For deoxyMb, we explicitly considered the overlap of the Soret band with the absorption of the dithionite ion.

RESULTS AND DISCUSSION

Experimental results

Figure 1 shows the Soret band absorption and CD spectra of deoxyMb, MbCN, and aquametMb. For the deoxystate, we observed a clear noncoincidence between absorption and CD spectra. The CD spectrum appears redshifted, much narrower, and even more asymmetric, compared to the absorption spectrum. A noncoincidence is also clearly recognizable for MbCN, but the CD band is now blueshifted with respect to the absorption band, and the difference between the profiles is less pronounced than what was observed for deoxyMb. For aquametMb, CD and absorption band profiles

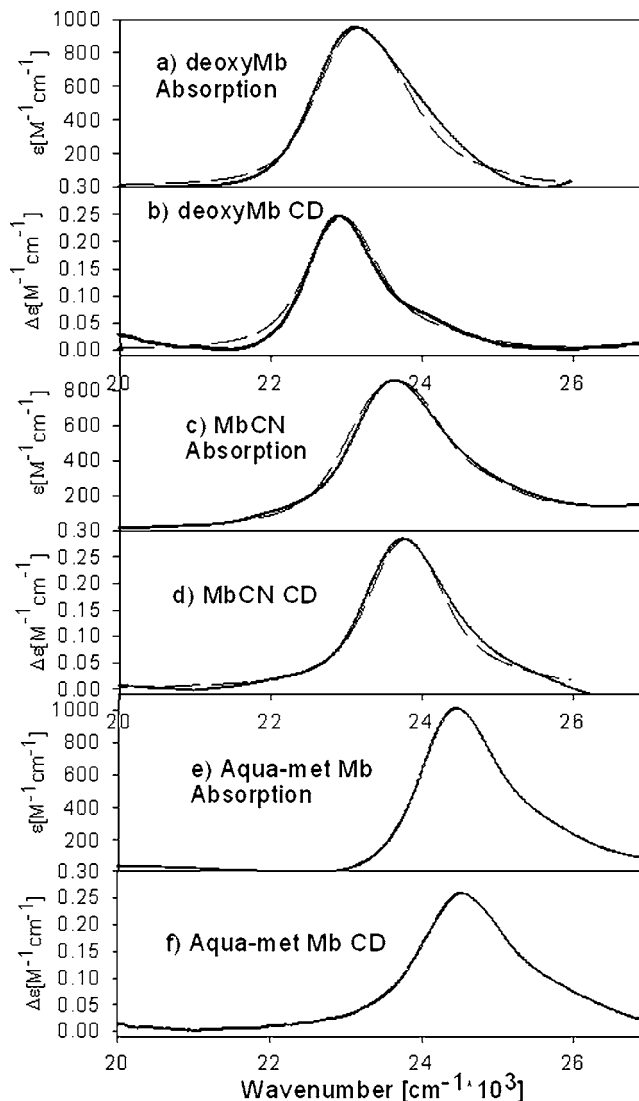


FIG. 1. Absorption spectra of (a) deoxyMb, (c) MbCN, and (e) aquametMb. CD spectra of (b) deoxyMb, (d) MbCN, and (f) aquametMb. Thick black line, experimental spectra and dashed line, simulated spectra.

are nearly identical. The only possible explanation for the noncoincidence observed for deoxyMb and MbCN is Soret band splitting. Apparently only one of the two components (B_x or B_y) carries substantial rotational strength induced by multiple electronic interactions with the heme environment.¹⁸

Analysis

To perform a quantitative analysis of the Soret bands of deoxyMb and MbCN, we utilized the vibronic coupling approach of Schweitzer-Stenner and Bigman,¹⁹ which was recently employed to analyze the Q -band spectra of various ferrocyanide derivatives to show that the splitting of the optical bands of heme proteins can arise from electronic and vibronic perturbations. If electronic perturbations are present, the electronic and magnetic transition dipole moments ($\pi = \mu, \mathbf{m}$) associated with the $0 \rightarrow 0$ B -band transition can be written as

$$\tilde{\pi}_{l',v_j}^B = \tilde{\pi}_{l,v_j}^{B_0} + \left(\sum_{\Gamma} \frac{\delta_{Q_l B_l}^{\Gamma}}{E_{l,v_j}^{B_0} - E_{k,v_j}^{Q_0}} \right) \tilde{\pi}_{k,v_j}^{Q_0}, \quad (1)$$

where $\tilde{\pi}_{l,v_j}^{B_0}$ ($\tilde{\pi}_{k,v_j}^{Q_0}$) is the respective moment (electronic or magnetic) of the transition into the unperturbed $B(Q)$ states ($l, k=x, y$) of the 50:50 states of Gouterman's four-orbital model,²⁰ which we use as a reference basis for the unperturbed heme. The subscript v_j denotes the vibrational quantum number of the j th oscillator, indicating that the described coupling occurs between equivalent vibrational levels of the corresponding states. $\tilde{\pi}_{l',v_j}^B$ is the dipole moment for the transition into the perturbed B state. It should be noted that $l'=x'y'$ can be different from the x, y directions of the unperturbed states, if perturbations lead to a rotation of the dipole moments.²¹ $\delta_{Q_l B_l}^{\Gamma}$ is the electronic coupling between Q_l and B_k ($l, k=x, y$) due to a perturbation of symmetry Γ , where Γ refers to the irreducible representations A_{1g} , B_{1g} , B_{2g} , and A_{2g} of the D_{4h} point group. $E_{k,v_j}^{Q_0}$ and $E_{l,v_j}^{B_0}$ are the eigenenergies of the unperturbed vibronic states $|Q_{0k}, v_j\rangle$ and $|B_{0l}, v_j\rangle$. The respective eigenenergies E_{l',v_j}^B ($l'=x', y'$) of the electronically perturbed states are written as

$$E_{l',v_j}^B = E_{l,v_j}^{B_0} + \frac{(\sum_{\Gamma} \delta_{Q_l B_l}^{\Gamma})^2}{E_{l,v_j}^{B_0} - E_{k,v_j}^{Q_0}}. \quad (2)$$

The summation runs over the representations A_{1g} , B_{1g} , B_{2g} , and A_{2g} . In the present study, we solely consider the electronic perturbation of A_{1g} and B_{1g} symmetries, for which l and k are either both x or y . Since $\delta_{Q_x B_x}^{A_{1g}} = \delta_{Q_y B_y}^{A_{1g}}$ and $\delta_{Q_x B_x}^{B_{1g}} = -\delta_{Q_y B_y}^{B_{1g}}$, splitting of $B_{x,y}^0$ arises if the respective perturbations are present, whereas no rotation occurs so that $l'=l=k$. This splitting is identical for all vibronic states of $B_{x,y}^0$ and $Q_{x,y}^0$.

Additional splitting of the $0 \rightarrow 0$ transition is caused by vibronic contributions which can be inferred from Eq. (3),

$$E_{l',0}^{B'} = E_{l',0}^B - \sum_j \frac{(\sum_{\Gamma''} c_{B_l' B_l'}^{\Gamma''}(j))^2}{\Omega_j^B} + \sum_{j'} \frac{(\sum_{\Gamma''} c_{Q_k' B_l'}^{\Gamma''}(j'))^2}{E_{l',0}^{B_0} - E_{k',0}^{Q_0} + \Omega_{j'}^B}, \quad (3)$$

where $E_{l',0}^{B'}$ denotes the eigenenergies of the vibronically and electronically perturbed B state, and $E_{l',0}^B$ and $E_{k',0}^Q$ are the energies of the electronically perturbed states $|B_{l'}, 0\rangle$ and $|Q_{k'}, 0\rangle$, respectively. Ω_j^B denote the vibrational energies of the j th vibration in the excited Q and B states, respectively. The parameter $c_{es}^{\Gamma''}(j)$ ($e, s=B_{l'}, Q_{k'}$ and $l', k'=x', y'$) denotes the vibronic coupling matrix elements of the j th vibrational mode of the heme macrocycle. Γ'' is the effective symmetry of the respective vibration in the presence of symmetry-lowering perturbations. The second term on the right of Eq. (3) describes the contribution from intrastate Franck-Condon (A_{1g}) and Jahn-Teller (B_{1g} and B_{2g}) couplings from the j th mode. The third term reflects contributions from interstate Herzberg-Teller coupling mostly of B_{1g} - and A_{2g} -type modes.¹⁹ Using the unperturbed D_{4h} symmetry as a reference system, $c_{es}^{\Gamma''}(j)$ can be expressed as

$$c_{es}^{\Gamma''}(j) = \langle e | \frac{\partial H_{el}}{\partial q_j^{\Gamma}} | s \rangle q_j^{\Gamma} + \sum_{\tilde{\Gamma}} \chi_{es}^{\tilde{\Gamma}}(j). \quad (4)$$

The first term in Eq. (4) describes the vibronic coupling of the j th mode of symmetry Γ in ideal D_{4h} symmetry, whereas the second term reflects additional vibronic coupling due to the vibronic perturbations, which adds terms related to the symmetry $\tilde{\Gamma} = \Gamma \otimes \Gamma_p$ to the vibronic coupling term. Γ_p is the symmetry of the symmetry-lowering vibronic perturbation. Equation (4) indicates that in a low symmetry, all coupling processes can contribute, e.g., if an A_{1g} mode is affected by B_{1g} or B_{2g} perturbations.

To account for the influence of electronic and vibronic perturbations on the vibronic sideband of the B band associated with the j th heme vibration, the respective dipole moments and eigenenergies are written as

$$\tilde{\pi}_{l',1_j}^{B'} = \frac{\sum_{\Gamma''} c_{B_l' B_l'}^{\Gamma''}(j)}{\Omega_j^B} \tilde{\pi}_{l',0_j}^{B'}, \quad (5a)$$

$$E_{l',v_j}^{B''} = E_{l',0_j}^B + \Omega_j^B - \frac{(\sum_{\Gamma''} c_{B_l' B_l'}^{\Gamma''}(j))^2}{\Omega_j^B} + (\sum_{\Gamma''} c_{Q_k' B_l'}^{\Gamma''}(j))^2 \times \left[\frac{1}{E_{l',0_j}^B - E_{k',0_j}^Q + \Omega_j^B} + \frac{2}{E_{l',0_j}^B - E_{k',0_j}^Q - \Omega_j^Q} \right]. \quad (5b)$$

Both equations account for Franck-Condon/Jahn-Teller coupling ($c_{B_l' B_l'}^{\Gamma''}$ terms) and interstate Herzberg-Teller coupling ($c_{Q_k' B_l'}^{\Gamma''}$ terms). Generally, it is assumed that only intrastate coupling affects the Soret band. However, strong interstate coupling due to A_{2g} modes can affect the eigenenergies. It should be emphasized in this context that for the sake of simplicity, we did not consider contributions due to thermal populations of excited vibrational states in the ground state.^{22,23}

To restrict the simulation of the Soret band absorption and CD profile of deoxyMb, we utilized the respective polarized resonance Raman spectra in Fig. 2, recorded with 442 nm excitation. The spectrum taken with parallel polarization is dominated by bands assignable to A_{1g} modes. The relative total intensities of these bands are in first order proportional to the respective coupling parameters $c_{B_l B_l}^{\Gamma}$. Thus, we neglect multimode effects which become relevant only for excitations on the high energy side of the Soret band.²⁴ We determined the depolarization ratios of the most prominent Raman lines. The respective values listed in Table I are close to the D_{4h} value of 0.125 for ν_4 but are significantly larger for the low wavenumber modes. This indicates the presence of asymmetric deformations.^{21,25} We performed a self-consistent simulation of B -band absorption and CD profile based on the relative intensities of the Raman bands listed in Table I and a Franck-Condon coupling parameter $c_{BB}^{A_{1g}} = 250 \text{ cm}^{-1}$ obtained for the ferrous state of horseradish peroxidase.²⁶ We first invoked B_{1g} type electronic splitting and adjusted the value of $\delta_{Q_l B_l}^{B_{1g}}$ so that the noncoincidence

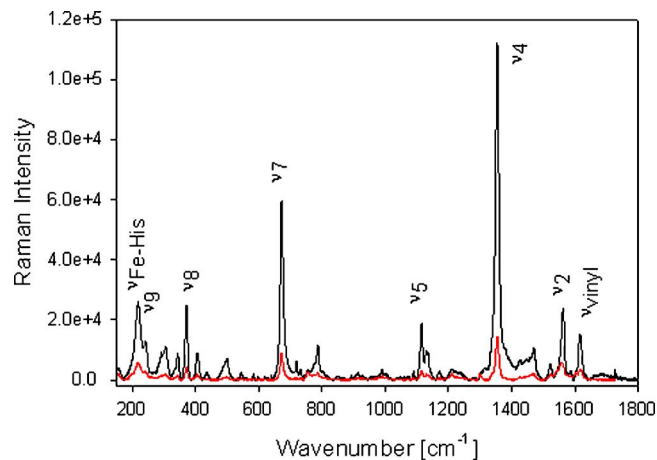


FIG. 2. (Color online) Polarized resonance Raman spectra of deoxymyoglobin measured with 442 nm excitation. Black solid line, spectrum taken with polarization parallel to the polarization of excitation. Red circle symbols, spectrum taken with polarization perpendicular to the polarization of excitation. The assignments of the major bands are indicated. The spectrum was corrected for self-absorption by using the method of Unger *et al.* (Ref. 38).

between the peak positions of absorption and CD profiles could be reproduced. The corresponding value for $\delta_{Q_i B_l}^{A_{1g}}$ was estimated from the Q_0 band intensity. Subsequently, we considered vibronic B_{1g} -type perturbations $c_{B_l B_l}^{B_{1g}}(j)$ for all modes listed in Table I. The respective values were obtained by calculating the Raman tensor of these modes so that their depolarization ratios were reproduced. For the simulation of the CD band, we assumed that only the low energy component (B_y) exhibits a rotational strength. This procedure yielded absorption and CD profiles that were in good qualitative agreement with the experimentally observed profiles, but the vibronic sideband was somewhat underestimated. Therefore, we scaled the vibronic coupling parameters by the same amount so that we obtained $c_{B_l B_l}^{A_{1g}}=300 \text{ cm}^{-1}$ for ν_4 . After some adjustment of $\delta_{Q_i B_l}^{B_{1g}}$, the simulation yielded a rather satisfactory reproduction of the band profiles. Finally, we allowed for some rotational strength for B_x . Thus, the dashed curves in Figs. 1(a) and 1(b) were obtained, which reproduce the experimental profile quite well. All coupling parameters used for this simulation are listed in Table II. For this simulation, we used Voigtian profiles for each subband of the vibronic progression. The spectral parameters are also listed in Table II. Our analysis reveals that the vibronic perturbations actually reduce the rather large electronic part of the splitting ($\sim 500 \text{ cm}^{-1}$) of the B_0 band ($0 \rightarrow 0$ transition) to

TABLE I. Depolarization ratios and relative intensities of resonance Raman bands measured with 442 nm excitation.

Raman active vibration	Depolarization ratio	Relative intensity
$\nu_{\text{Fe-His}}$	0.21	0.45
ν_9	0.2	0.1
ν_8	0.17	0.14
ν_7	0.15	0.44
ν_4	0.13	1.0
ν_2	0.13	0.21
ν_{vinyl}	0.22	0.16

TABLE II. Spectral and coupling parameters used for the simulation of the absorption and CD band profiles of the Soret band of deoxyMb.

(a) Electronic and spectral parameters		
E_B		23 224 cm^{-1}
$\delta_{Q_i B_l}^{B_{1g}}$		800 cm^{-1}
ΔE_{B_0}		187 cm^{-1}
Γ_B		300 cm^{-1}
σ_B		300 cm^{-1}
(b) Vibronic coupling parameters		
Vibrational mode	$c_{B_l B_l}^{A_{1g}}$	$c_{B_l B_l}^{B_{1g}}$
$\nu_{\text{Fe-His}}$ (221 cm^{-1})	135	70
ν_9 (231 cm^{-1})	70	35
ν_8 (370 cm^{-1})	84	30
ν_7 (670 cm^{-1})	149	50
ν_4 (1355 cm^{-1})	300	26
ν_2 (1563 cm^{-1})	103	
ν_{vinyl} (1620 cm^{-1})	99	44

189 cm^{-1} . The respective splittings of the vibronic sidebands are significantly larger (400–500 cm^{-1}) (Supplementary Information, Table E1)²⁷ because the vibronic influence on the respective energy values is less pronounced. The splitting of the $0 \rightarrow 0$ transition is affected by the vibronic contributions from all modes [Eq. (3)], whereas the $0 \rightarrow 1_j$ transition in first order solely probes the vibronic coupling of the corresponding j th vibration. The interference between electronic and vibronic splittings is reversed for the Q band. As demonstrated by Levantino *et al.*²⁸ for cytochrome *c*, the $0 \rightarrow 0$ splitting is generally larger than the respective $0 \rightarrow 1$ splittings. This opposite influence of vibronic coupling on B - and Q -band splittings was already predicted by Schweitzer-Stenner and Bigman.¹⁹

To check the validity of our model, we applied it to the absorption and CD profiles observed for MbCN [Figs. 1(c) and 1(d)]. This ligation state of myoglobin has been investigated earlier by using the resonance Raman excitation profiles and depolarization ratio dispersions of some resonance Raman lines to simulate the absorption spectrum and the polarized absorption spectra,²⁴ which Eaton and Hochstrasser obtained for MbCN crystals.²⁹ We now used the spectral and coupling parameters reported in this study to simulate the Soret absorption and CD band profile of MbCN. Only minor changes of the parameters were necessary to obtain the very satisfactory reproduction of the experimental profiles [dashed lines in Figs. 1(c) and 1(d)]. The blueshift of the CD spectrum results from the fact that the sign of $c_{Q_i B_l}^{A_{1g}}$ is negative, so that B_x and B_y change their positions. This success of our approach strongly underscores its validity.

It is necessary to emphasize in this context that the technically elegant time correlator approach which Šrajer *et al.*¹⁴ employed to describe the vibronic part of the Soret profile in terms of the coupling parameters associated with the dominant resonance Raman bands is not applicable in the presence of electronic and vibronic perturbations, which lead to different band profiles for B_x and B_y .²⁴

Comparison with literature

Woody and co-workers investigated the CD spectrum of heme proteins including myoglobin.^{18,30,31} Hsu and Woody modeled the Soret band of myoglobin and hemoglobin derivatives by considering the electronic coupling between the heme and aromatic residue side chains.¹⁸ Their calculations yielded rotational strengths of opposite sign and slightly different magnitudes for the two B -state components, which give rise either to a small positive Cotton band coincident with the absorption band, if the band splitting was much smaller than the bandwidth, or a couplet, if the band splitting was larger than the bandwidth, as observed for ferricytochrome c .¹⁶ None of these prediction are apparently in agreement with our experimental data. Hsu and Woody invoke a 3 nm splitting between the two polarizations which corresponds to 175 cm^{-1} , without considering vibronic components, and very close to 189 cm^{-1} that we discovered here for the B_0 band ($0 \rightarrow 0$ transition). The calculation of Hsu and Woody was based on the assumption that the transition dipole moments of the B -band transition are aligned with the N–Fe–N lines. Changes of this orientation can drastically affect the CD spectrum. A rotation of the transition dipole moments can be caused by B_{2g} type or the combined presence of A_{2u} and B_{1u} perturbations.²¹ Blauer *et al.* presented a more refined model by calculating the rotational strength of the Soret band transitions for the cytochrome c undecapeptide.³² The authors extended the model of Hsu and Woody by additionally considering $n \rightarrow \pi^*$ and $\pi \rightarrow \pi^*$ transitions of the peptide groups as well as $\pi \rightarrow \pi^*$ transitions of imidazole rings. Their most sophisticated model, which considered the polarizability of the peptide groups and heme transition dipole orientation from quantum chemical calculations, yielded, indeed, two clearly different, positive contributions for the two Soret band components. This is in qualitative, though not quantitative, agreement with the result of our analysis, from which we obtained a larger discrepancy between B_x and B_y .

Franzen recently proposed a somewhat different approach for rationalizing the band shape of the absorption band and MCD signal of deoxyMb,¹⁵ namely, vibronic coupling between the excited B states and the charge transfer state ($a_{2u}d_\pi$) of the ferrous high spin iron, which is excited by a charge transfer transition in the near infrared (band III at 13 100 cm^{-1}). Based on resonance Raman excitation profiles measured in the band III region,³³ he developed a model that invokes vibronic coupling via the lowest frequency mode of the B_{1g} block at 150 cm^{-1} as the dominant source of Soret band splitting. As a theoretical tool, the author utilized the old perimeter model, which describes the π electrons of the heme macrocycle as particles on a ring. Different electronic states are characterized by different magnetic quantum numbers of the angular momentum operator \hat{L}_z . Apparently, this is a very convenient model for explaining MCD spectra, but it does not account for the fact that the $|g\rangle \rightarrow |Q_0\rangle$ transition is actually not totally forbidden, owing to an imbalance of Gouterman's 50:50 states. Our main objection to Franzen's theoretical treatment, however, concerns his treatment of vibronic coupling. He describes the change of the electronic

potential by using an operator $(\partial V/\partial R)\Delta R$, where V is the electronic potential. ΔR is the deformation induced by the aforementioned B_{1g} mode, i.e., ν_{18} in the notation of Abe *et al.*³⁴ The corresponding matrix elements $(2\pi)^{-1} \langle E_\pm | \partial V/\partial R | CT_\pm \rangle \Delta R$ (E_\pm and CT_\pm are the two components of the degenerate heme and iron state, respectively) were estimated by modeling a rhombic deformation of the electronic ground state associated with ν_{18} and by using the electronic wave functions of the perimeter model. The model yielded $\mp k\Delta R^2/2$, where k is a force constant. Franzen argued that the difference between these two values (i.e., $k\Delta R^2$) is a measure of the excited state's (B -band) splitting. Strictly speaking this approach is incorrect. The above vibronic matrix element reflects interstate coupling, which affects eigenenergies only in second order, for which one obtains the term $(2\pi)^{-1} (\langle E_\pm | \partial V/\partial R | CT_\pm \rangle \Delta R)^2 / \Delta E$. Hence, no splitting is obtained in agreement with the well established notion that neither Herzberg-Teller nor Jahn-Teller coupling can lift the degeneracy of E_u states if the heme is in D_{4h} symmetry.^{21,35} As shown by Schweitzer-Stenner and Bigman,¹⁹ the splitting of such states by, e.g., B_{1g} modes requires a vibronic perturbation $\partial V^{B_{1g}}/\partial Q^{B_{1g}}$, which arises from the variations of electronic perturbations $V^{B_{1g}}$ by B_{1g} -type vibrational modes. In our approach, we considered the vibronic perturbations of B_{1g} symmetry associated with A_{1g} modes, which add B_{1g} -type intrastate vibronic coupling to the Franck-Condon coupling of A_{1g} modes, thus affecting the splitting of the B band.

The earlier and still mostly accepted explanation of the Soret band profile of deoxyMb is that of Šrajcar *et al.*,¹⁴ who mapped a Gaussian distribution of heme doming onto the eigenenergy of the Soret band by using the simple relationship,

$$E_B(Q) \cong E_{B_0} + bQ^2, \quad (6)$$

where E_{B_0} is the energy of the degenerated B state for a planar heme, b is a coupling constant, and Q was identified with the iron out-of plane displacement, which is the main local coordinate of the lowest frequency doming coordinate γ_9 .³⁶ Šrajcar *et al.* obtained a b value of 2570 $\text{cm}^{-1}/\text{\AA}^2$. The corresponding energy shift for a displacement of 0.5 \AA is 642.5 cm^{-1} .¹⁴ It is intriguing to convert b into a physically, more meaningful parameter by assuming that it reflects some type of electronic coupling between the a_{2u} highest occupied molecular orbital of the heme and the d_z^2 orbital of the iron. For deoxyMb, the energy difference is approximately 10 000 cm^{-1} . Thus, by utilizing second order perturbation theory, one obtains a coupling energy of 2535 cm^{-1} . This value is very high. The model of Šrajcar *et al.* was used subsequently to model the temperature dependence of the Soret band of sperm whale myoglobin.³⁷ Surprisingly, this yielded a much lower value for b , namely, $b=710 \text{ cm}^{-1}/\text{\AA}^2$, which corresponds to a coupling strength of 700 cm^{-1} , certainly a much more reasonable value. The reason for this discrepancy remains unclear. Ormos *et al.* used Eq. (6) to explore the relationship between the displacement parameter Q and the CO rebinding at different temperatures between 100 and 260 K.¹³ They found that the latter does not depend on the former and concluded that the displacement of the iron atom

(i.e., heme doming) is not a kinetic coordinate. Apparently, the results of our analysis offer another solution, namely, that Q has much less of an influence on the Soret band profile. The electronic and vibronic perturbations invoked in our theory are not expected to exhibit a significant temperature dependence, even though some variations of vibronic coupling associated with low frequency modes might occur due to the depopulation of higher vibrational states and the concomitant decrease of $1 \rightarrow 2$ transitions at low temperatures. We therefore propose that in contrast to the proposal by Ormos *et al.*, Q is a kinetically relevant parameter but not a main spectral determinant of the Soret band.

SUMMARY

The noncoincidence between the CD and the absorption band profiles of deoxyMb and MbCN indicates a splitting of the excited B state. We employed the vibronic coupling model of Bigman and Schweitzer-Stenner¹⁹ to simulate both the absorption and CD spectra of both myoglobin derivatives. The result of our analysis suggests that the splitting is caused by a rather large electronic deformation which is reduced by vibronic coupling induced by vibronic perturbations of the same symmetry. Based on the success of our simulation, we argue that heme doming (the Fe out-of-plane displacement) is not the decisive coordinate for the Soret band of deoxyMb. This conclusion resolves a conflict between the observation that the temperature dependence of the kinetics of CO rebinding is uncorrelated with concomitant changes of the Soret band and many experimental data which suggest that the heme doming determines the activation enthalpy of ligand binding.

Note added in proof. Our analysis of band splitting neglects the possibility that the electronic part could stem from an electric field with different components along the x - and y -transition dipole moments of the B -band. Manas *et al.*³⁹ have argued that the respective potential which couples ground and excited B -state, can cause substantial splitting owing the strong dipole moment of the B -band transition. This argument was questioned by Schweitzer-Stenner and Bigman¹⁹, but their group theoretical argumentation might be problematic. A final proof of a possible influence of the internal electric field in heme proteins on the splitting of these transitions requires a comparison of Q - and B -band splitting,³⁸ which has not yet been achieved on a quantitative level. With respect to the present paper, however, we like to emphasize that our data would not allow us to discriminate between the considered B_{2g} -type electronic perturbations (which can be related to the electric quadrupole moment²⁸) and a direct influence of electric field components. The conclusions drawn in this study are therefore independent of the interpretation of the obtained electronic perturbation value.

ACKNOWLEDGMENTS

Financial support was provided from a grant from the National Science Foundation (No. MCB-0318749) to one of the authors (R.S.S.).

- ¹H. Frauenfelder, G. Petsko, and D. Tsernoglou, *Nature (London)* **280**, 558 (1979).
- ²R. H. Austin, K. W. Beeson, L. Eisenstein, H. Frauenfelder, and I. C. Gunsalus, *Biochemistry* **14**, 5355 (1975).
- ³A. Ansari, J. Berendzen, S. F. Bowne, H. Frauenfelder, I. E. T. Iben, T. B. Sauke, E. Shyamsunder, and R. D. Young, *Proc. Natl. Acad. Sci. U.S.A.* **82**, 5000 (1985).
- ⁴F. Parak, E. W. Knapp, and D. Kucheida, *J. Mol. Biol.* **161**, 177 (1982).
- ⁵G. U. Nienhaus and R. D. Young, *Encyclopedia Appl. Phys.* **15**, 163 (1996).
- ⁶W. Doster, S. Cusack, and W. Petry, *Nature (London)* **337**, 754 (1989).
- ⁷P. M. Fenimore, H. Frauenfelder, B. H. McMahon, and F. G. Parak, *Proc. Natl. Acad. Sci. U.S.A.* **99**, 16047 (2002).
- ⁸H. Frauenfelder, F. Parak, and R. D. Young, *Annu. Rev. Biophys. Biophys. Chem.* **17**, 451 (1988).
- ⁹A. Ansari, J. Berendzen, D. Braunstein *et al.*, *Biophys. Chem.* **26**, 337 (1987).
- ¹⁰G. H. Nienhaus, J. R. Mourant, and H. Frauenfelder, *Proc. Natl. Acad. Sci. U.S.A.* **89**, 2902 (1992).
- ¹¹P. J. Steinbach, A. Ansari, J. Berendzen *et al.*, *Biochemistry* **30**, 3988 (1991).
- ¹²V. Šrajcar and P. M. Champion, *Biochemistry* **30**, 7390 (1991).
- ¹³P. Ormos, S. Szaraz, A. Cupane, and G. U. Nienhaus, *Proc. Natl. Acad. Sci. U.S.A.* **95**, 6762 (1998).
- ¹⁴V. Šrajcar, K. T. Schomaker, and P. M. Champion, *Phys. Rev. Lett.* **57**, 1267 (1986).
- ¹⁵S. Franzen, *J. Phys. Chem. B* **106**, 10482 (2002).
- ¹⁶I. Dragomir, A. Hagarman, C. Wallace, and R. Schweitzer-Stenner, *Biophys. J.* **92**, 989 (2007).
- ¹⁷W. Jentzen, E. Unger, G. Karvounis, J. A. Shelnut, W. Dreybrodt, and R. Schweitzer-Stenner, *J. Phys. Chem.* **100**, 14184 (1996).
- ¹⁸M. C. Hsu and R. W. Woody, *J. Am. Chem. Soc.* **93**, 3515 (1971).
- ¹⁹R. Schweitzer-Stenner and D. Bigman, *J. Phys. Chem. B* **105**, 7064 (2001).
- ²⁰M. Gouterman, *J. Chem. Phys.* **30**, 1139 (1959).
- ²¹R. Schweitzer-Stenner, *Q. Rev. Biophys.* **22**, 381 (1989).
- ²²K. Schomaker, O. Bangcharoenpaupong, and P. M. Champion, *J. Chem. Phys.* **80**, 70 (1984).
- ²³A. Cupane, M. Cammarata, L. Cordone, M. Leone, E. Vitrano, N. Engler, and F. Parak, *Eur. Biophys. J.* **34**, 881 (2005).
- ²⁴R. Schweitzer-Stenner, A. Cupane, M. Leone, C. Lemke, J. Schott, and W. Dreybrodt, *J. Phys. Chem. B* **104**, 4754 (2000).
- ²⁵M. Z. Zgierski and M. Pawlikowski, *Chem. Phys.* **65**, 335 (1982).
- ²⁶Q. Huang and R. Schweitzer-Stenner, *J. Raman Spectrosc.* **36**, 363 (2005).
- ²⁷See EPAPS Document No. E-JCPSA6-127-001735 for the lists the splittings of the vibronic sidebands. This document can be reached through a direct link in the online article's HTML reference section or via the EPAPS homepage (<http://www.aip.org/pubservs/epaps.html>).
- ²⁸M. Levantino, Q. Huang, A. Cupane, M. Laberge, A. Hagarman, and R. Schweitzer-Stenner, *J. Chem. Phys.* **123**, 054508 (2005).
- ²⁹W. A. Eaton and R. M. Hochstrasser, *J. Chem. Phys.* **49**, 985 (1968).
- ³⁰H. Drucker, L. L. Campbell, and R. W. Woody, *Biochemistry* **9**, 1519 (1970).
- ³¹C. Keifl, N. Sreerama, R. Haddad, L. Sun, W. Jentzen, Y. Lu, Y. Qiu, J. A. Shelnut, and R. W. Woody, *J. Am. Chem. Soc.* **124**, 3385 (2002).
- ³²G. Blauer, N. Sreerama, and R. W. Woody, *Biochemistry* **32**, 6674 (1993).
- ³³S. Franzen, S. E. Wallace-Williams, and A. P. Shreve, *J. Am. Chem. Soc.* **124**, 7146 (2002).
- ³⁴M. Abe, T. Kitagawa, and Y. Kyogoku, *J. Chem. Phys.* **69**, 4526 (1978).
- ³⁵J. A. Shelnut, *Chem. Phys.* **74**, 6644 (1981).
- ³⁶P. Kozłowski, T. G. Spiro, and M. Z. Zgierski, *J. Phys. Chem. B* **104**, 10659 (2000).
- ³⁷A. Cupane, M. Leone, and E. Vitrano, *Eur. Biophys. J.* **21**, 385 (1993).
- ³⁸E. Unger, U. Bobinger, W. Dreybrodt, and R. Schweitzer-Stenner, *J. Phys. Chem.* **97**, 9956 (1993).
- ³⁹E. S. Manas, J. M. Vanderkool, and K. A. Sharp, *J. Phys. Chem. B* **103**, 6344 (1999).